ELSEVIER

Progress in Surface Science 74 (2003) 141–159

Progress in SURFACE SCIENCE

www.elsevier.com/locate/progsurf

Identification of defect sites on oxide surfaces by metastable impact electron spectroscopy

S. Wendt, Y.D. Kim, D.W. Goodman *

Department of Chemistry, Texas A&M University, P.O. Box 30012, College Station, TX 77842-3012, USA

Abstract

In this review, thin films of SiO_2 on Mo(1 1 2) and MgO(1 0 0) on Mo(1 0 0) have been characterized using metastable impact electron and ultraviolet photoelectron spectroscopies (metastable impact electron spectroscopy (MIES) and ultraviolet photoelectron spectroscopy). The electronic and chemical properties of the thin films are identical to those of the corresponding bulk oxides. For different prepared defective SiO_2 surfaces, additional features are observed in the band-gap region. These features arise from vacancies or excess oxygen and are consistent with theoretical predictions of additional occupied states in the band-gap due to point defects. Extended defect sites on SiO_2 and MgO are identified using MIES by a narrowing of the O(2p) features with a reduction in the density of extended defect sites. MIES of adsorbed Xe (MAX) is also used to estimate the density of extended defect sites. Furthermore, it is shown that CO is an appropriate probe molecule for estimating the defect density of MgO surfaces. Upon Ag exposure, the change in the work function of a low defect MgO(1 0 0) versus a high defect surface is markedly different. For a sputter-damaged MgO(1 0 0) surface, an initial decrease of the work function was found, implying that small Ag clusters on this surface are electron deficient. In contrast, for SiO_2 no significant change of the work function upon Ag exposure with increasing defect density was observed. On MgO(1 0 0), the presence of defect sites markedly alter the electronic and chemical properties of supported Ag clusters. Such a strong influence of defect sites was not found for Ag clusters on SiO_2.

Keywords: MgO; SiO_2; Xenon; Carbon monoxide; Silver; Surface defects; Metastable impact electron spectroscopy (MIES); Ultraviolet photoelectron spectroscopy (UPS)

* Corresponding author. Tel.: +1-979-845-0214; fax: +1-979-845-6822.
E-mail address: goodman@mail.chem.tamu.edu (D.W. Goodman).

0079-6816/$ - see front matter © 2003 Elsevier Ltd. All rights reserved.
doi:10.1016/j.progsurf.2003.08.011

1. Introduction

A molecular-level understanding of surface phenomena in metal oxides is important to a variety of technologies including electronic devices, heterogeneous catalysis, electrochemistry, and geochemistry. Although wide band-gap oxides, such as MgO, SiO_2 and Al_2O_3, are of particular importance, studies of these materials utilizing surface sensitive charged particle probes are complicated, because of sample charging. It has been shown that oxide thin films, supported on refractory metal surfaces, provide a convenient method for circumventing difficulties related to charging [1]. Using a suitable substrate, epitaxially grown oxide thin films of MgO, Al_2O_3, and TiO_2 have been synthesized that exhibit essentially the same electronic and chemical properties of the corresponding bulk single crystals [1–4]. In recent studies, SiO_2 single crystalline thin films have been synthesized on a Mo(1 1 2) surface [5,6].

The identification and characterization of defect sites on oxide surfaces is important in the manufacture of electronic devices, where defects can cause significant degradation [7]. Moreover, defects on oxide surfaces play a pivotal role in heterogeneous catalysts as nucleation sites for metal nanoclusters and as sites for reaction. Metastable impact electron spectroscopy (MIES) is an extremely surface sensitive technique that uses exited helium atoms with thermal energy as a surface probe [8]. MIES provides such superior surface sensitivity that quite small concentration of defect sites on the surface can also be detected. It is noteworthy that ultraviolet photoelectron spectroscopy (UPS) is much less sensitive than MIES with respect to F/F^+-centers and extended defects [9]. On the other hand, the unique surface sensitivity of MIES is restricted to wide band-gap materials or metals with very low work functions [8].

The existence of point defects gives rise to additional states within the band-gap that can be readily identified with optical absorption measurements [10], electron energy loss spectroscopy (EELS) [11,12] and UPS. MIES, however, has been shown to be particularly suitable, especially if the defect density is very low. The identification of extended defects, such as steps and grain boundaries, is more complex, since no distinct additional features derived from extended defects are generally observed. However, a broadening of the O(2p) band has been suggested by theoretical studies [13].

A possible route to identify extended defects is the use of probe molecules that uniquely interact with defect sites. Finding appropriate probe molecules to titrate extended defects is therefore a key to understanding the properties of defects on oxide surfaces. Appropriate probe molecules used in conjunction with MIES provide insight into the nature of the defect sites. On MgO(1 0 0), for instance, CO molecules adsorbs selectively on defect sites [1,3,14,15]. CO adsorption experiments on MgO(1 0 0) allow the titration of defect sites and thus provide a method for distinguishing between high and low defective MgO(1 0 0) thin films. Moreover, MIES of adsorbed Xe (MAX) [16] can be used to titrate extended defects. In MAX, the substrate signals are completely quenched and only the Xe-peaks appear, due to the extremely high surface sensitivity of MIES. Therefore, MAX provides very accurate

information regarding the binding energies, energy positions, and width of the Xe 5p states. Using MAX, the local work function can be estimated very accurate, even for surfaces for which the application of photoemission of adsorbed Xe (PAX) is difficult, due to the superposition of Xe-peaks and substrate features [16]. Furthermore, metal clusters can be used as a probe for defect sites, since metal clusters on oxide surfaces interact preferentially with the defects [17,18], and, in turn, can be modified electronically and chemically [19,20]. To illustrate this, work function measurements and adsorption studies have been carried out on Ag clusters adsorbed on SiO_2. Ag was chosen, because of its relevance to a variety of catalytic processes.

In this review, a methodology for identifying several types of defects on crystalline MgO and SiO_2 surfaces is described. The lineshapes of MIES spectra in conjunction with low energy electron diffraction (LEED) data, CO-temperature programmed desorption (TPD) spectra, and MIES spectra of adsorbed Xe significantly change in the presence of defects. Upon Ag exposure, the work function also changes as a function of defect density. Combinations of these experimental techniques are shown to be effective for identification of several kinds of defects. This methodology allows one to distinguish between extended and point defects on oxide surfaces, and is suitable for use with other wide band-gap oxides.

2. Experimental

The experiments were carried out in an ultrahigh vacuum (UHV) system (base pressure 1×10^{-10} Torr) consisting of two interconnected chambers. One chamber is equipped with an ion-gun for sputtering, LEED and TPD. The second chamber contains Auger electron spectroscopy (AES), X-ray photoelectron spectroscopy (XPS) and MIES/UPS. MIES/UPS spectra were measured simultaneously using a cold-cathode discharge source [21,22] that provides both ultraviolet photon and metastable He 2^3S ($E^* = 19.8$ eV) atoms with thermal kinetic energy. Metastable and photon contributions to the signal were separated by a time-of-flight method using a mechanical chopper. MIES and UPS spectra were acquired with the photon/metastable beams incident at 45° with respect to the surface normal and utilizing a double pass cylindrical mirror analyzer (CMA). The resolution of the analyzer, estimated from the width of the Fermi edge, is $\approx$0.4 eV. The work functions were estimated from the low-energy onset of the secondary electrons in the UPS spectra.

For wide band-gap materials or metals with very low work functions, Auger-deexcitation (AD) is the dominant mechanism that leads to the MIES signal. In this case, a plot of the intensity of the ejected electrons versus their kinetic energies yields the surface density of states (SDOS) for the topmost layer of the surface [8]. In the following spectra, all binding energies are referenced to the Fermi level of the Mo substrate. The Mo samples, used as substrates for the thin oxide films, were cleaned by repeated flashing to 2200 K; the sample cleanliness was verified with AES. The LEED pattern of the clean Mo surfaces showed intense spots and low background intensity. The Ag evaporation source consisted of a tungsten filament wrapped with

an ultrahigh purity (99.99%) Ag wire. Before Ag deposition, the evaporation source was thoroughly outgassed and calibrated using AES.

3. Preparation and electronic structure of oxide thin films

3.1. Ultrathin crystalline SiO_2 films on Mo(1 1 2)

To prepare a low defect SiO_2 thin film [5,6], Si was deposited on Mo(1 1 2) at room temperature and annealed at 800 K in 1×10^{-7} Torr oxygen. Subsequently, the film was typically annealed at 1200 K for several minutes in 1×10^{-7} Torr oxygen. LEED for the SiO_2 films, synthesized as above, showed a c(2×2) periodicity, indicating the formation of a well-ordered SiO_2 network. For these SiO_2 thin films, Si^{4+} features were evident at 76 eV in the AES spectra with no Si^0 features at ≈90 eV, indicating that the Si is completely oxidized. Using the attenuation of the Mo peaks in AES, the thickness of the film was estimated to be 0.4–0.7 nm. The described preparation methodology is adapted from the work of Freund and coworkers [5,6].

In Fig. 1, MIES spectra for SiO_2 thin films taken after a brief anneal in oxygen at 1200 K (5 min) and after an extended anneal (60 min) at the same temperature are compared. The spectra show a major feature at 8 eV with a shoulder at 7 eV and a smaller feature at 11 eV. The features at 6–8 eV correspond to the O(2p) non-bonding states, and the peak at 11 eV to the Si–O bonding state [23,24]. After the extended anneal at 1200 K the features of the MIES spectra are narrower and the shoulder at 7 eV is more pronounced, indicating that the surface becomes more ordered upon annealing. The LEED results corroborate this interpretation. Annealing of the sample in oxygen at 1200 K leads to an increase of the LEED spot intensities and to a decrease of the background intensity. It should be noted that a

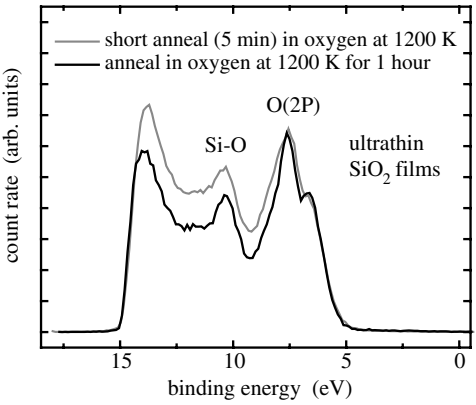

Fig. 1. MIES spectra collected from SiO_2 thin film, prepared at room temperature and annealed in 1×10^{-7} Torr oxygen on Mo(1 1 2). Only time for final anneal in oxygen at 1200 K was different as indicated. The thickness of film was ≈0.5 nm.

shoulder at 7 eV is evident for amorphous SiO_2 using He(II)-UV-light [23,24], and that calculated density of states show fine structure for the polymorphs of SiO_2, e.g. β-tridymite, α-cristobalite and β-cristobalite within this energy range [25].

The UPS spectrum for this SiO_2 thin film (not shown) is similar to the MIES spectrum, i.e., the spectrum is also dominated by the O(2p) and the Si–O features. In the UPS data, additional features between 0–4 eV are apparent (see Fig. 3(b)). These features, with low intensities, arise from the Mo(1 1 2) substrate. It should be emphasized that MIES has been shown to be sensitive only to the topmost surface layer, whereas UPS integrates over the surface and near-surface region [8].

The MIES/UPS spectra for these SiO_2 thin films are similar to previously published photoemission spectra for SiO_2 bulk crystals [24], indicating that the electronic properties of the SiO_2 thin films with a thickness of 0.4–0.7 nm are essentially identical to those of bulk SiO_2. In addition, STS data for SiO_2 thin films with a thickness of 0.5 nm show bulk like electronic properties corroborating this conclusion [26].

3.2. *MgO(1 0 0) thin films on Mo(1 0 0)*

To prepare thin MgO films, Mg was deposited on Mo(1 0 0) in an O_2 background of 1×10^{-7} Torr at 600 K. The thickness of the thin films was varied within the range of 2–15 monolayers (ML). In all cases, AES did not show a metallic Mg peak at 44 eV, whereas the Mg^{2+} peak at 32 eV was distinctly visible [27], indicating that Mg was completely oxidized. The LEED pattern of these thin films exhibited a (1×1)-periodicity with diffuse spots and relatively high background intensity, indicating that the "as-grown" MgO thin films are rough and poorly ordered. These results are consistent with recent results that showed a sharp (1×1)-LEED pattern from the as-grown MgO films only when the thickness of the film was greater than 30 ML [14].

Previous LEED investigations found that subsequent annealing of the MgO thin films does not lead to improvement in the LEED patterns [27]. In fact, when the thickness of the MgO films was less than ≈5 ML, the diffuse (1×1)-LEED pattern remained unchanged upon annealing at 1150 K. In contrast, a sharp (1×1)-LEED pattern could be obtained by annealing a MgO thin film grown at 600 K with a thickness of ≈15 ML.

In Fig. 2, MIES data for an as-grown MgO(1 0 0) films taken before and after annealing at 1150 K are compared. For the clean MgO surface, the O(2p) feature appears at 5.5 eV below the Fermi level. No F/F^+ defect features at 1–2.5 eV were observed with MIES, indicating that the number of F/F^+-centers is relatively small [9]. The full-width-half-maximum (FWHM) of the O(2p) peak decreased from 3.2 to 2.5 eV upon annealing. Narrowing of the O(2p) band, indicating that the surface becomes more ordered upon annealing, is consistent with the LEED results, i.e., the (1×1)-spots are sharper after annealing. These results agree with previous atomic force microscopy (AFM) investigations of MgO single crystals, where the roughness of the MgO single crystal surfaces could be significantly reduced by annealing the crystal at high temperatures ($T > 1250$ K) [28].

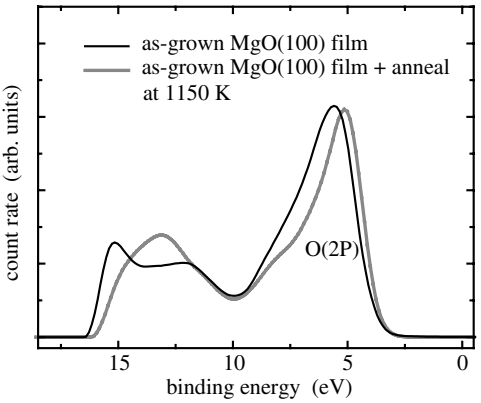

Fig. 2. MIES spectra collected from as-grown MgO film on Mo(1 0 0) before and after annealing at 1150 K. Thickness of film was ≈3.5 nm (15 ML).

For MgO(1 0 0) films with a thickness of 30 ML or greater, surface charging was observed during electron spectroscopic measurement [1]. However, on MgO(1 0 0) films with a thickness of only 15 ML no surface charging occurs [1]. On the other hand, recent scanning tunnelling spectroscopy (STS) studies in combination with UPS and EELS show that bulk-like electronic properties of MgO thin films on Ag(1 0 0) develop within the first 2–3 ML (≈0.5–0.8 nm) [29]. Hence, low defect MgO(1 0 0) films with a thickness of 15 ML are appropriate models for a bulk MgO(1 0 0) surface, yet suitable for electron spectroscopic measurements.

4. Identification of point defects on silica thin films

In previous optical spectroscopy investigations on defective SiO_2 various absorption and luminescence bands were found [7,30–36]. Theoretical studies, carried out to understand the optical absorption and photoluminescence spectra of SiO_2 [7,37–43], have shown that additional occupied and unoccupied states are present in the band-gap region [37], when various defect sites (oxygen vacancies or excess oxygen) are present. These defect sites are considered to be responsible for the experimentally observed color centers.

If defect sites on SiO_2 surfaces correspond to occupied states within the band-gap, MIES should identify these defect states. An additional occupied state in the band-gap, which is not present on low defect SiO_2 surfaces, is observed for a defective SiO_2 surface prepared by depositing excess Si onto a well-ordered SiO_2 surface at room temperature followed by oxidation at 800 K (Fig. 3(a)). After annealing at 1050 K in oxygen, the band-gap state disappears, indicating that the anneal reduces the number of the related defect sites. Given that the defective surface in Fig. 3 was created by oxygen treatment at 800 K, it is reasonable to assume that the number of oxygen vacancies on this surface is not high. Furthermore, no Si^0 was detected with AES, consistent with the number of

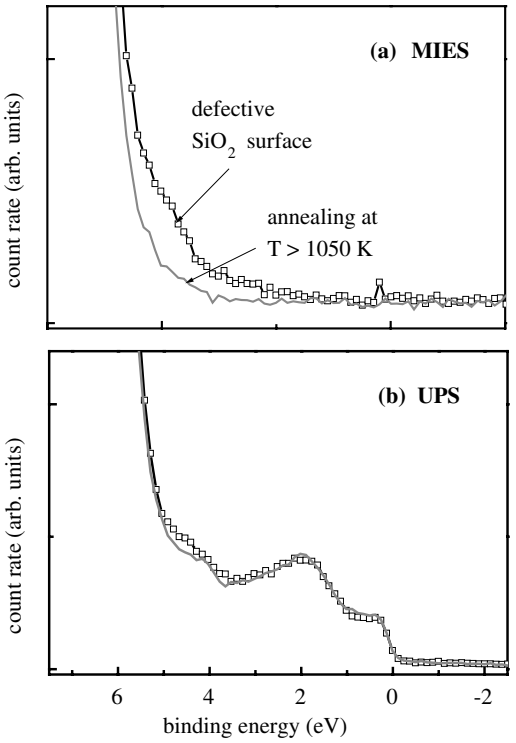

Fig. 3. (a) Enlarged view of MIES spectra in low binding energy region for defective SiO_2 film before and after annealing at 1050 K. (b) Corresponding UPS spectra. Defective film was prepared by deposition of Si onto well-ordered SiO_2 film at room temperature, followed by oxidation at 800 K. Further annealing at 1050 K results in disappearance of defect state.

oxygen vacancies being low. Therefore, it is likely that defect sites other than oxygen vacancies, such as peroxyl bridge, peroxyl radical, or non-bridging oxygen [37], are responsible for the appearance of the band-gap states in Fig. 3(a).

In contrast to MIES, no additional electronic state induced by defect sites can be clearly identified by UPS (Fig. 3(b)). Furthermore, the UPS spectra consist of contributions from the SiO_2 film, as well as features from the underlying Mo(1 1 2) substrate that overlap the band-gap states from various defect sites of SiO_2. This superposition of the Mo(1 1 2) features and the defect states complicate the unambiguous identification of defect states in the band-gap using UPS.

States in the band-gap region also appear after deposition of Si onto SiO_2 at room temperature (Fig. 4). Si deposition onto SiO_2 at room temperature introduces features in the MIES spectrum similar to those found for the defective SiO_2 surfaces of Fig. 3. A SiO_2 thin film damaged by 3 kV-electron-beam yields a virtually identical spectrum (not shown). Si deposition onto SiO_2 and also electron-beam treatment of a low defect SiO_2 surface can create an oxygen-depleted SiO_2 surface with an electronic structure essentially identical to a surface with oxygen vacancies. However, it is noteworthy

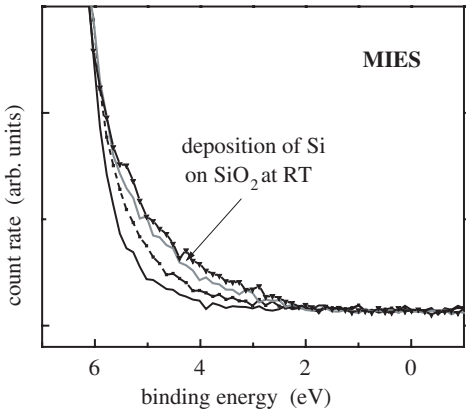

Fig. 4. Enlarged view of MIES spectra in low binding energy part for SiO_2 thin film as function of Si deposition at 300 K.

that Si(III)-(7×7) surface also displays electronic states in this energy region [44,45], therefore deposition of Si at room temperature and electron-beam treatment of a low defect SiO_2 surface leading to Si clusters cannot be excluded. For MgO(1 0 0), additional features in the band-gap as measured by EELS, and has been assigned to oxygen vacancies (e.g., neutral F centers) [12]. At the same time, Mg deposition-induced features in the band-gap of MgO(1 0 0) also had been identified using MIES [46]. Furthermore, it is known that high energy electron-beam treatments of MgO(1 0 0) surfaces selectively remove oxygen atoms from the surface, creating F/F^+ centers [9].

5. MIES of adsorbed Xe (MAX) to probe extended defect sites

5.1. High and low defective MgO(1 0 0) surfaces

Another technique enabling the identification of defect sites is MIES of adsorbed Xe (MAX) [16]. In Fig. 5(a), the MIES spectrum for the vacuum-annealed MgO(1 0 0) surface is compared with that from a comparably prepared surface with adsorbed Xe. The MIES spectrum for the adsorbed Xe-monolayer was acquired in a Xe background pressure of 5×10^{-5} Torr at a sample temperature of 80 K. Xe on the surface typically gives rise to sharp doublet features originating from the $5p_{1/2}$ and $5p_{3/2}$ states of adsorbed Xe atoms [47]. In general, the $5p_{3/2}$ signal splits into two sublevels causing broadening of the $5p_{3/2}$-peak [48]. As shown in Fig. 5(a), the MIES spectrum collected for Xe/MgO yields a sharp doublet feature from the Xe 5p states. The O(2p) peak from the substrate completely disappears indicating that the surface is almost completely covered by Xe. The relatively high intensity of the $5p_{3/2}$ peak is probably due to the high cross-section of this state for the AD process. A similar ratio of intensities of the $5p_{1/2}$ and $5p_{3/2}$ levels was found in a previous MIES study of Xe-multilayers [49].

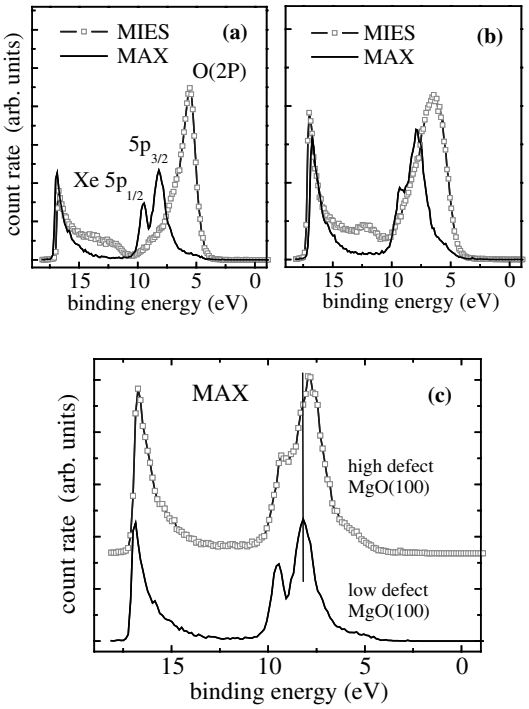

Fig. 5. MIES and MIES of adsorbed Xe (MAX) for MgO surfaces with (a) low and (b) high defect densities. In (c), MAX spectra for both surfaces are compared. High defect surface was prepared by deposition of Mg in O_2 background of 1×10^{-7} Torr at room temperature. Low defective surface was prepared by deposition of Mg in O_2 background of 1×10^{-7} Torr at 600 K, followed by multiple anneals at 1150 K (thickness $\approx$15 ML).

Fig. 5(b) shows MIES spectra for bare and Xe-adsorbed MgO surfaces grown at 300 K without further annealing. The broader O(2p) feature in Fig. 5(b) compared to that of Fig. 5(a) is consistent with this surface having a greater density of extended defects. For the MgO surface, grown at 300 K without annealing, the $5p_{1/2}$ and $5p_{3/2}$ levels of Xe are broader compared with those of the vacuum-annealed MgO surface. The broad Xe-peaks in MIES indicate that the adsorption sites for the Xe atoms are more heterogeneous than for a vacuum-annealed MgO(1 0 0) surface. These results show that the valence band structure for an adsorbed Xe-monolayer can be used to estimate the uniformity of the surface. The MAX spectrum of the high defect MgO surface shows shoulders at lower binding energies with respect to the Xe 5p states of the low defect surface (Fig. 5(c)). Based on the assumption that the Xe-5p level is pinned to the vacuum-level of the surface [50,51], the local work function of the defect sites in the 300 K-grown MgO(1 0 0) films should be higher than that of a relatively defect-free MgO(1 0 0) surface. However, the work function of the 300 K-grown MgO(1 0 0) film determined by the on-set of the secondary electrons in UPS is lower than that of the vacuum-annealed MgO(1 0 0) film, in disagreement with the MAX-results. The results of Fig. 5(c) show that the Xe 5p levels in MAX do not always

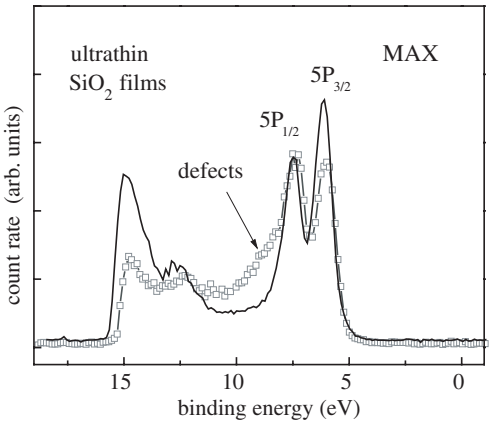

Fig. 6. MAX for low and high-defect SiO_2 films on Mo(1 1 2).

reflect the surface local work functions. Therefore, the use of Xe 5p energy position to determine the local work functions is problematic for defective oxide surfaces.

5.2. High and low defective SiO_2 surfaces

MAX spectra for the high and low defect SiO_2 surfaces are presented in Fig. 6. The SiO_2 surfaces were produced by annealing the 800 K-prepared film at 1050 and 1200 K, respectively. For the 1200 K-annealed SiO_2 surface, sharp doublet features from the Xe $5p_{1/2}$ and $5p_{3/2}$ levels are observed, indicating a high degree of surface homogeneity. In contrast, the 1050 K-annealed film shows a shoulder at higher binding energies in addition to the Xe doublet features. Such a shoulder is not visible for defective MgO surfaces, and most likely, results from Xe atoms adsorbed at extended defect sites. Electronic structures of adsorbed Xe atoms on regular and defect sites can be different, possibly due to the different local electronic structures of defect sites with respect to those of regular sites, and thus the 5p orbitals of Xe atoms on regular and defect sites can appear at various binding energies [16]. It is noteworthy that photoemission of adsorbed Xe (PAX) has been widely used for the characterization of heterogeneous surfaces, in particular, bimetallic surfaces [50]. In any case, from the relative intensity of this shoulder with respect to those of the sharp doublet features, the extended defect density for the 1050 K-annealed SiO_2 surface is estimated to be approximately 20–30%.

6. CO as probe molecule for MgO(1 0 0) surfaces

6.1. CO TPD from various MgO thin films

It has been shown that CO adsorbs selectively on defect sites of MgO(1 0 0) surfaces at 90 K [1,3,14,15], suggesting that CO can be used as a probe molecule to

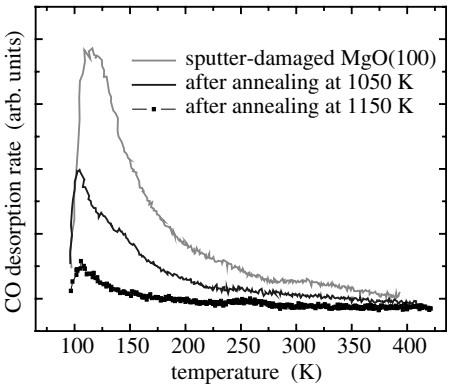

Fig. 7. CO TPD from MgO(1 0 0) surfaces with different defect densities.

titrate certain defect sites. In Fig. 7, CO TPD spectra from various MgO(1 0 0) films are compared. A CO TPD spectrum acquired from a sputter-damaged surface exhibits a CO desorption feature at 120 K. After annealing the sputter-damaged surface to 1050 K, the intensity of the CO desorption peak decreases. Subsequent annealing to 1150 K reduces the intensity of the CO desorption peak even further. Obviously, the number of defect sites, which can be assessed by CO molecules, is smaller after annealing. These spectra confirm that CO can be used as a probe molecule to titrate defect sites on MgO(1 0 0) surfaces.

6.2. CO adsorption on as-grown MgO(1 0 0) film

To clarify the TPD results, MIES/UPS spectra were collected as a function of CO exposure on various MgO surfaces [1]. At first, the MgO(1 0 0) film grown at a sample temperature of 600 K (thickness ≈15 ML) was exposed to CO at 90 K (Fig. 8). Note that this film exhibited a diffuse (1×1)-LEED pattern, and a relatively broad O(2p) feature in the MIES spectrum, indicating that the surface is not well-ordered. Fig. 8(a) shows the MIES spectra collected as a function of CO exposure and Fig. 8(b) shows the corresponding difference spectra. At the early stage of CO exposure, the intensity of the O(2p) peak decreases markedly. The intensity of the O(2p) shows an attenuation of approximately 35% upon CO exposures of 5 L or more. Further CO exposure leads to a more slowly attenuating O(2p) feature in the MIES spectra. Additional peaks at 10, 12.4 and 14.6 eV develop in the MIES spectra during CO exposure (Fig. 8(b)). As the CO exposure increases, the peak at 12.4 eV shifts to 12.0 eV. Further CO exposure leads to a gradual shift of the peaks at 12.0 and 14.6 eV to lower binding energies. The attenuation of the O(2p) peak saturates at CO exposures between 5 and 10 L, whereas the CO-induced peaks continue to shift with higher CO exposures to lower binding energies.

The CO induced features are also visible in the corresponding UPS spectra (not shown). The overall changes of the UPS spectra upon CO exposure are similar to those of the MIES spectra in Fig. 8.

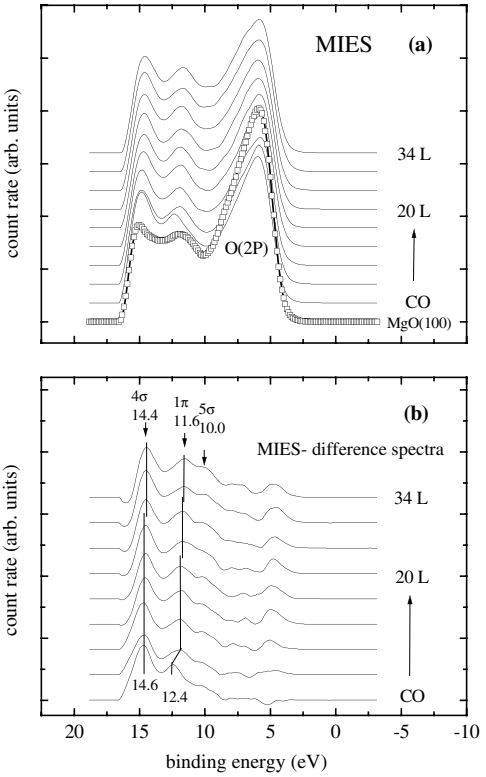

Fig. 8. (a) MIES spectra taken as function of CO exposure from as-grown MgO(1 0 0) film ≈15 ML in thickness. (b) Difference spectra of Fig. 9(a). Before subtracting MgO-spectrum from CO/MgO spectrum, MgO spectrum was appropriated attenuated taking into account CO-induced damping of MgO features.

The three CO-peaks at 10, 12.4, and 14.6 eV in the MIES spectra (Fig. 8) are assigned to the 5σ, 1π, and 4σ orbitals of CO. In the gas phase, the separation between the 5σ and 1π levels is 2.9 eV, whereas on transition metal surfaces, the 1π and 5σ levels typically overlap, because of the shift of the 5σ orbital [52]. On MgO(1 0 0) surfaces, the 5σ and 1π levels are separated by 1.6 eV in both the MIES and UPS spectra. A separation of 1.6 eV for the 1π and 4σ peaks was also observed for ZnO(1 0 1 0) [53]. The large separation between the 5σ and 1π orbitals on both oxide surfaces is likely a result of weak interaction of the 5σ level with the oxide surfaces compared to this interaction on a transition-metal surface.

The shifts of the CO-peaks with increasing CO coverage are consistent with a strong lateral interaction between the CO molecules. Thus, it is likely that the CO coverage at the adsorption site or sites is relatively high at 90 K. However, the O(2p) attenuation in the MIES spectra is only 35% upon a 5 L or higher exposure of CO at 90 K, indicating that the overall coverage of CO on the surface at 90 K is not high. Note that the completion of the CO monolayer should result in a 100% attenuation of the O(2p) feature, because MIES is exclusively sensitive to the outermost surface

layer. From these results, we conclude that CO adsorption takes place only on a specific area of the surface, most probably extended defect sites such as step edges and corners.

6.3. CO on annealed MgO(1 0 0) surface

In a further experiment, the vacuum annealed MgO(1 0 0) surface of the same thickness was investigated using MIES and UPS. After annealing the as-grown MgO(1 0 0) surface at 1150 K, the MIES spectra were collected during CO exposure (Fig. 9). No change of the spectra could be observed even with a CO background pressure of 1×10^{-6} Torr. Consequently, no adsorption of CO takes place at 90 K on the MgO(1 0 0) surface after the MgO(1 0 0) thin film has been annealed at 1150 K. These results are in agreement with a recent TPD study using a bulk MgO single crystal where no CO TPD peaks were found above 90 K [15]. Furthermore, the CO-induced c(4×2)-LEED structure is observed on the MgO(1 0 0) single crystal at 40 K, whereas above 55 K, no superstructure spots were observed, indicating that desorption of the first CO monolayer takes place at this temperature [54]. Thus, the adsorptive properties of CO on a MgO(1 0 0) single crystal are identical to those of the vacuum annealed MgO(1 0 0) film. Therefore, the well-ordered MgO(1 0 0) thin films possess essentially identical chemical properties like in situ cleaved single crystals. This conclusion is also supported by the virtually identical D_2O-TPD spectra from both surfaces [3,55].

The results presented in this section clearly show that CO is an appropriate molecule to titrate defect sites on MgO(1 0 0) and are consistent with previous investigations. NO also has been used to probe certain defect sites on MgO(1 0 0) surfaces [7,56,57], however, a recent study has raised questions regarding its efficacy for doing so [3].

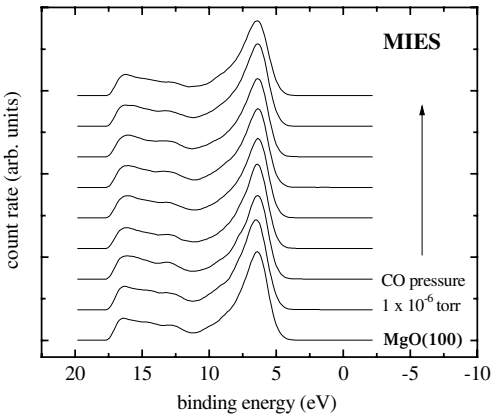

Fig. 9. MIES spectra taken from vacuum-annealed MgO(1 0 0) film as function of CO exposure ($P(\mathrm{CO}) = 1 \times 10^{-6}$ Torr, $T = 90$ K). Film thickness of vacuum-annealed MgO(1 0 0) film was ≈15 ML.

7. Interaction of Ag with various oxide surfaces

7.1. Interaction of Ag with MgO(1 0 0)

It is generally accepted that interactions of metals with defective oxide surfaces are stronger than those with non-defect oxide surfaces. Therefore, metal clusters decoration could be suitable as a probe for defect sites. Using MIES/UPS various defective oxide surfaces upon metal deposition have been investigated. For Ag deposition onto a sputtered MgO(1 0 0) surface an unusual change in the work function was found [58].

For all MgO(1 0 0) surfaces with varying defect density, the O(2p) feature in the MIES/UPS spectra attenuates upon Ag exposure. With increasing Ag coverages the Ag-induced features appear, as previously observed in MIES/UPS studies by Kempter and coworkers [59]. In addition, the low-energy onset of the secondary electrons shifts upon Ag exposure, indicating a change in the work function, whose variation as a function of the Ag coverage is summarized in Fig. 10. On the as-grown and also on the vacuum-annealed MgO(1 0 0) film, the work function gradually changes with increasing Ag exposure from ≈3 to 4 eV (Fig. 10, trace a)). Note that the vacuum-annealed MgO(1 0 0) has a significantly reduced number of extended defect sites in comparison to the as-grown MgO surfaces, as shown in Sections 3 and 5. Hence, extended defects do not play a significant role in determining the work function, since the work function change upon Ag exposure for both MgO(1 0 0) surfaces is virtually identical.

In contrast to the results from the as-grown and vacuum-annealed MgO(1 0 0) surfaces, the work function varies with Ag deposition in an unusual manner, if the vacuum-annealed MgO(1 0 0) surface is first sputtered and then annealed to 600 K (Fig. 10, trace b). In this case, the work function initially decreases upon Ag depo-

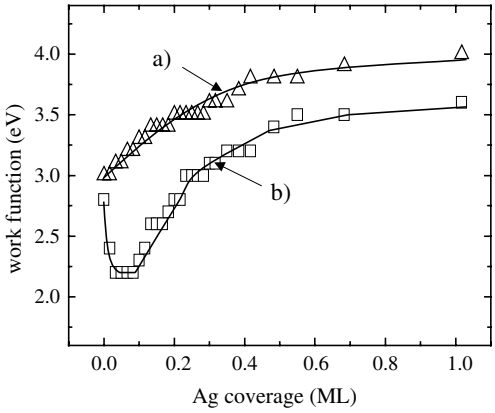

Fig. 10. Work function for MgO(1 0 0) surfaces with (a) low and (b) high density of point defects as function of Ag exposure. High defect MgO surface was produced by sputtering of vacuum-annealed MgO surface. Work function change was estimated from low-energy onset of the secondary electrons in UPS spectra.

sition. The sputtering most likely creates point defects, such as neutral and charged F- and V-centers that are presumably responsible for the initial decrease of the work function upon Ag deposition. This explanation is somewhat different from those presented by Kempter and coworkers who considered extended defects or Mg vacancies (V-centers) to be responsible for the formation of electron deficit Ag clusters at low Ag coverages [59]. However, by varying the number of extended defects, the initial decrease in the work function upon Ag deposition was not observed, indicating that extended defects are not responsible for this decrease at low Ag coverages.

After sputtering the vacuum-annealed MgO(1 0 0) surface, no F/F^+-center features within the band-gap region were detected with MIES, indicating that the number of the F/F^+-centers did not increase significantly [3]. Furthermore, F/F^+-centers should not oxidize Ag to $Ag^{\delta+}$, since the electron affinity of a F/F^+-center is rather low [60]. All together, it is unlikely that F/F^+-centers are responsible for the decrease of the work function at low Ag coverages. Oxygen vacancies created by sputtering can form F^{2+}-centers, features not observed with MIES. The electron affinity of the F^{2+}-centers, on the other hand, is sufficiently high to withdraw electron density from Ag to form $Ag^{\delta+}$ [60]. Moreover, it cannot be excluded that Mg vacancies (such as V/V^--centers) could lead to $Ag^{\delta+}$; however, previous studies have shown that sputtering preferentially removes oxygen from oxide surfaces, leading to an increase in the relative number of O-vacancies compared to Mg-vacancies on the sputter-damaged MgO surfaces [61].

Our results suggest that Ag atoms selectively interact with point defects on the surface at low Ag coverages. These results are consistent with several theoretical studies as well as with an AFM study for Pd on MgO(1 0 0) [19,60,62]. All these studies show that there is a strong interaction between adsorbed metal atoms and point defects on MgO. The work function measurements presented in Fig. 10 indicate that Ag clusters on the sputter-damaged MgO(1 0 0) surface are to a degree positively charged at low Ag coverages.

Using CO as a probe molecule, we also investigated the chemical properties of Ag clusters on various MgO surfaces [58]. It was found that, in the case of a sputter damaged MgO(1 0 0) surface after deposition of a small amount of Ag, the amount of adsorbed CO increases by a factor of two compared to a vacuum-annealed MgO(1 0 0) surface. Since CO does not adsorb on bulk Ag at 70 K [63,64], it is unlikely to adsorb on relatively large Ag clusters at 80 K. However, Ag atoms at the Ag–MgO interface are chemically modified compared to bulk Ag, due to rehybridization of the Ag-valence band with the O(2p) band of MgO [65]. This electronic modification of the Ag atoms at the Ag–MgO interface gives rise to the increased stability of CO. Thus, the larger amounts of CO that adsorb on low Ag coverages on the sputter-damaged MgO(1 0 0) can be related to the electron deficient nature of Ag clusters on such a defective MgO(1 0 0) surface, consistent with the work function data.

7.2. Ag Adsorption on various silica thin films

In contrast to MgO, upon Ag deposition on SiO_2, no enhanced charge transfer between Ag and SiO_2 in the presence of defect sites was found [66]. The work

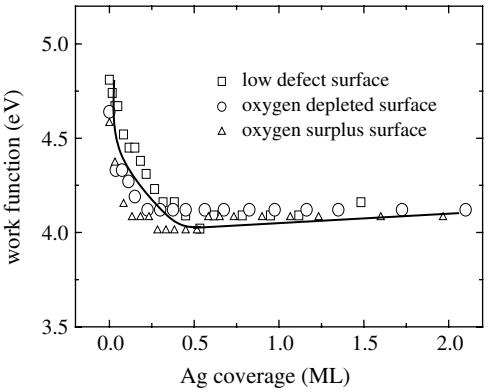

Fig. 11. Work function for various defective SiO_2 surfaces as function of Ag exposure. The oxygen-depleted surface was prepared by Si deposition on SiO_2; the oxygen-surplus surface was prepared by oxygen treatment of a Si/SiO_2 surface at 800 K.

function data for high and low-defect SiO_2 films upon Ag exposure are almost identical (Fig. 11). A comparison with the corresponding data for MgO(1 0 0) (Fig. 10) reveals that the changes of the work function as a function of the Ag coverage for SiO_2 films of varying defect density are much less pronounced. From these data, it is concluded that the bonding between Ag and defect sites on SiO_2 is primarily covalent, results consistent with recent theoretical studies. In these theoretical investigations, it has been shown that transition metals such as Pd, and Cu and various point defects on SiO_2 form strong covalent bonds [67,68], whereas for MgO, enhanced charge transfer between point defects and adsorbed metals has been suggested [19,60,69].

8. Conclusion

Various techniques have been used to characterize low and highly defective MgO(1 0 0) and SiO_2 surfaces. The electronic and chemical properties of both oxide thin films are identical to those of the corresponding bulk oxides indicating that these films can be used as model catalysts and catalyst supports.

Using MIES, additional features for various defect sites on SiO_2 surfaces are observed in the band-gap region, whereas UPS shows only minor features that can be related to the presence of defect sites. These results illustrate that low densities of defect sites on oxides surfaces not detectable using other surface science techniques can be measured with MIES.

Narrowing of the O(2p) band upon sample treatment (annealing or annealing in oxygen, respectively) indicates that the oxide surface becomes more homogeneous, i.e., the density of extended defects decreases. Extended defects on MgO(1 0 0) can also be detected using CO as a probe molecule. At 90 K CO adsorbs on the as-grown MgO(1 0 0) film, whereas no CO is adsorbed on a vacuum-annealed MgO(1 0 0) film.

Furthermore, MIES of adsorbed Xe as a function of the surface defect density shows that Xe atoms yield features at unique binding energies, confirming that MIES of adsorbed Xe can be used as well to identify extended defects.

The work function changes of various MgO(1 0 0) films as a function of Ag coverage imply that the electronic properties of small Ag clusters can be significantly altered in the presence of point defects. The chemical properties of Ag clusters interacting with point defects are also quite different from those on defect-free MgO surfaces. This finding underlines the significant role of point defects in defining the catalytic properties of oxide-supported metal clusters. For SiO_2 films, analogous experiments do not show significant changes of the work function as a function of the Ag coverage. This result is interpreted as due to little significant charge transfer between Ag and SiO_2 suggesting that the bonding between Ag and defect sites is primarily covalent.

Acknowledgements

Funding for this work was provided by the Department of Energy, Office of Basic Energy Sciences, Division of Chemical Sciences, and the Robert A. Welch Foundation, and the Texas Advanced Technology Program under Grant no. 010366-0022-2001. Tao Wei is acknowledged for fruitful discussions.

References

[1] Y.D. Kim, J. Stultz, D.W. Goodman, Surf. Sci. 506 (2002) 228.
[2] D.W. Goodman, J. Vac. Sci. Technol. A 14 (1996) 1526.
[3] Y.D. Kim, J. Stultz, D.W. Goodman, Langmuir 18 (2002) 3999.
[4] C. Xu, D.W. Goodman, Chem. Phys. Lett. 265 (1997) 341.
[5] T. Schroeder, A. Hammoudeh, M. Pykavy, N. Magg, M. Adelt, M. Baumer, H.J. Freund, Solid State Elect. 45 (2001) 1471.
[6] T. Schroeder, M. Adelt, B. Richter, M. Naschitzki, M. Baumer, H.J. Freund, Surf. Rev. Lett. 7 (2000) 7.
[7] G. Pacchioni, L. Skuja, D.L. Griscom, Defects in SiO_2 and related dielectrics: Science and technology, NATO Science Series, 2002.
[8] Y. Harada, S. Masuda, H. Ozaki, Chem. Rev. 97 (1997) 1897.
[9] A. Kolmakov, J. Stultz, D.W. Goodman, J. Chem. Phys. 113 (2000) 7564.
[10] Y. Chen, R.T. Williams, W.A. Sibley, Phys. Rev. 182 (1969) 960.
[11] M.C. Wu, C.M. Truong, D.W. Goodman, Phys. Rev. B 46 (1992) 12688.
[12] C. Tegenkamp, H. Pfnűr, W. Ernst, U. Malaske, J. Wollschlager, D. Peterka, K.M. Schroeder, V. Zielasek, M. Henzler, J. Phys.: Cond. Mat. 11 (1999) 9943.
[13] L.N. Kantorovich, A.L. Shluger, P.V. Sushko, A.M. Stoneham, Surf. Sci. 444 (2000) 31.
[14] Z. Dohnalek, G.A. Kimmel, S.A. Joyce, P. Ayotte, R.S. Smith, B.D. Kay, J. Phys. Chem. B 105 (2001) 3747.
[15] R. Wichtendahl, M. Rodriguez-Rodrigo, U. Hartel, H. Kuhlenbeck, H.J. Freund, Phys. State Sol. A 173 (1999) 93.
[16] Y.D. Kim, J. Stultz, T. Wei, D.W. Goodman, J. Phys. Chem. B 107 (2003) 592.
[17] G. Haas, A. Menck, H. Brune, J.V. Barth, J.A. Venables, K. Kern, Phys. Rev. B 61 (2000) 11105.

[18] M. Baumer, M. Frank, M. Heemeier, R. Kuhnemuth, S. Stempel, H.J. Freund, Surf. Sci. 454 (2000) 957.
[19] U. Heiz, W.D. Schneider, J. Phys. D—Appl. Phys. 33 (2000) R85.
[20] Y.D. Kim, J. Stultz, T. Wei, D.W. Goodman, J. Phys. Chem. B 106 (2002) 6827.
[21] W. Mausfriedrichs, M. Wehrhahn, S. Dieckhoff, V. Kempter, Surf. Sci. 237 (1990) 257.
[22] W. Mausfriedrichs, S. Dieckhoff, V. Kempter, Surf. Sci. 249 (1991) 149.
[23] T.H. DiStefano, D.E. Eastman, Phys. Rev. Lett. 27 (1971) 1560.
[24] A. Dipomponio, A. Continenza, L. Lozzi, M. Passacantando, S. Santucci, P. Picozzi, Solid State Commun. 95 (1995) 313.
[25] A.L. Ivanovskii, Russ. J. Inorg. Chem. 46 (2001) S15.
[26] B.-K. Min, A. Santra, D.W. Goodman, 2002, unpublished results.
[27] M.C. Wu, J.S. Corneille, C.A. Estrada, J.W. He, D.W. Goodman, Chem. Phys. Lett. 182 (1991) 472.
[28] S.S. Perry, H.I. Kim, S. Imaduddin, S.M. Lee, P.B. Merrill, J. Vac. Sci. Technol. A 16 (1998) 3402.
[29] S. Schintke, S. Messerli, M. Pivetta, F. Patthey, L. Libioulle, M. Stengel, A. De Vita, W.D. Schneider, Phys. Rev. Lett. (2001) 8727, art-276801.
[30] A.N. Trukhin, M. Goldberg, J. Jansons, H.J. Fitting, I.A. Tale, J. Non-Cryst. Sol. 223 (1998) 114.
[31] A.J. Miller, R.G. Leisure, V.A. Mashkov, F.L. Galeener, Phys. Rev. B 53 (1996) R8818.
[32] H. Nishikawa, E. Watanabe, D. Ito, Y. Ohki, Phys. Rev. Lett. 72 (1994) 2101.
[33] H. Nishikawa, Y. Miyake, E. Watanabe, D. Ito, K.S. Seol, Y. Ohki, K. Ishii, Y. Sakurai, K. Nagasawa, J. Non-Cryst. Sol. 222 (1997) 221.
[34] M. Guzzi, F. Pio, G. Spinolo, A. Vedda, C.B. Azzoni, A. Paleari, J. Phys.: Cond. Mat. 4 (1992) 8635.
[35] R. Boscaino, M. Cannas, F.M. Gelardi, M. Leone, J. Phys.: Cond. Mat. 8 (1996) L545.
[36] R. Boscaino, M. Cannas, F.M. Gelardi, M. Leone, Phys. Rev. B 54 (1996) 6194.
[37] G. Pacchioni, G. Ierano, Phys. Rev. B 57 (1998) 818.
[38] G. Pacchioni, G. Ierano, A.M. Marquez, Phys. Rev. Lett. 81 (1998) 377.
[39] G. Pacchioni, G. Ierano, Phys. Rev. B 56 (1997) 7304.
[40] G. Pacchioni, G. Ierano, J. Non-Cryst. Sol. 216 (1997) 1.
[41] G. Pacchioni, G. Ierano, Phys. Rev. Lett. 79 (1997) 753.
[42] T. Uchino, M. Takahashi, T. Yoko, Phys. Rev. Lett. 86 (2001) 5522.
[43] T. Uchino, M. Takahashi, T. Yoko, Phys. Rev. Lett. 86 (2001) 4560.
[44] S. Nishigaki, M. Sugihara, M. Ohta, S. Fuki, K. Matsuo, T. Noda, Jpn. J. Appl. Phys. 25 (1986) L501.
[45] S. Masuda, H. Ishii, Y. Harada, Solid State Comm. 82 (1992) 587.
[46] J. Günster, J. Stultz, S. Krischok, D.W. Goodman, S. Stracke, V. Kempter, J. Vac. Sci. Technol. A 17 (1999) 1657.
[47] J. Hulse, J. Kuppers, K. Wandelt, G. Ertl, Appl. Surf. Sci. 6 (1980) 453.
[48] M. Scheffler, K. Horn, A.M. Bradshaw, K. Kambe, Surf. Sci. 80 (1979) 69.
[49] D.M. Oro, P.A. Soletsky, X. Zhang, F.B. Dunning, G.K. Walters, Phys. Rev. A 49 (1994) 4703.
[50] K. Wandelt, Appl. Surf. Sci. 111 (1997) 1.
[51] K. Wandelt, J. Vac. Sci. Technol. A 2 (1984) 802.
[52] G. Ertl, J. Kuppers, Low Energy Electrons and Surface Chemistry, VCH Verlagsgesellschaft Mbh, Weinheim, 1985.
[53] J. Lin, P. Jones, J. Guckert, E.I. Solomon, J. Am. Chem. Soc. 113 (1991) 8312.
[54] P. Audibert, M. Sidoumou, J. Suzanne, Surf. Sci. 273 (1992) L467.
[55] S.I.U. Ahmed, S.S. Perry, O. El Bjeirami, J. Phys. Chem. B 104 (2000) 3343.
[56] J.A. Rodriguez, T. Jirsak, J.Y. Kim, J.Z. Larese, A. Maiti, Chem. Phys. Lett. 330 (2000) 475.
[57] J.A. Rodriguez, T. Jirsak, M. Perez, L. Gonzalez, A. Maiti, J. Chem. Phys. 114 (2001) 4186.
[58] Y.D. Kim, J. Stultz, T. Wei, D.W. Goodman, J. Phys. Chem. B 106 (2002) 6827.
[59] P. Stracke, S. Krischok, V. Kempter, Surf. Sci. 473 (2001) 86.
[60] A.M. Ferrari, G. Pacchioni, J. Phys. Chem. 100 (1996) 9032.
[61] V.E. Henrich, P.A. Cox, The Surface Science of Metal Oxides, Cambridge University Press, Cambridge, 1994.
[62] M. Komiyama, T. Shimaguchi, Surf. Interf. Anal. 32 (2001) 189.

[63] U. Burghaus, H. Conrad, Surf. Sci. 333 (1995) 116.
[64] W. Hansen, M. Bertolo, K. Jacobi, Surf. Sci. 253 (1991) 1.
[65] S. Altieri, L.H. Tjeng, G.A. Sawatzky, Phys. Rev. B 61 (2000) 16948.
[66] Y.D. Kim, T. Wei, S. Wendt, D.W. Goodman, Langmuir 19 (2003) 7932.
[67] N. Lopez, F. Illas, G. Pacchioni, J. Am. Chem. Soc. 121 (1999) 813.
[68] G. Pacchioni, N. Lopez, F. Illas, Faraday Discuss. (1999) 209.
[69] S. Abbet, A. Sanchez, U. Heiz, W.D. Schneider, A.M. Ferrari, G. Pacchioni, N. Rosch, J. Am. Chem. Soc. 122 (2000) 3453.